

## A Fluorescent Responsive Hybrid Nanogel for Closed-Loop Control of Glucose

Weitai Wu, Ph.D.,<sup>1,2,3,4</sup> Shoumin Chen, B.S.,<sup>2,3,4</sup> Yumei Hu, M.D.,<sup>2,3,4</sup> and Shuiqin Zhou, Ph.D.<sup>1</sup>

### Abstract

#### Background:

The concept of closed-loop control of glucose, in which continuous glucose sensing is coupled to a fully automated insulin delivery device, without human input, has been an attractive idea for diabetes management. This study presents a new class of hybrid nanogels that can integrate glucose sensing and glucose-responsive insulin release into a single nano-object.

#### Methods:

Zinc oxide@poly[N-isopropylacrylamide (NIPAM)-acrylamide (AAM)- 2-aminomethyl-5-fluorophenylboronic acid (FPBA)] hybrid nanogels were synthesized and investigated for size, morphology, volume phase transition, photoluminescence properties, and *in vitro* insulin release under different glucose concentrations. Glucose sensing was performed both in phosphate-buffered saline (PBS) and in blood samples. The insulin release in PBS of varying glucose levels, as well as a stepwise treatment between two glucose levels (126.0 and 270.0 mg/dl), was performed to test the glucose-responsive insulin release ability of the hybrid nanogels.

#### Results:

Zinc oxide@poly(NIPAM-AAM-FPBA) hybrid nanogels can sensitively and selectively detect glucose in highly reproducible fluorescent signals over the clinically relevant glucose concentration range of 18–540 mg/dl. The glucose-responsive volume phase transition of the nanogels can further regulate the release of the preloaded insulin. The insulin release from the nanogels exhibits the slowest rate (~5% released in 76 h) at a normal glucose level (108.0 mg/dl) but becomes quicker and quicker as the glucose increases to higher and higher levels.

#### Conclusions:

The rationally designed hybrid nanogel can optically signal the glucose level with high sensitivity and selectivity and simultaneously regulate the insulin release rate in response to the glucose reading, which shows a promising concept toward the development of a miniaturized closed-loop glycemic control system.

*J Diabetes Sci Technol* 2012;6(4):892-901

**Author Affiliations:** <sup>1</sup>Department of Chemistry, College of Staten Island, Graduate Center, City University of New York, Staten Island, New York; <sup>2</sup>State Key Laboratory for Physical Chemistry of Solid Surfaces, College of Chemistry and Chemical Engineering, Xiamen University, Xiamen, China; <sup>3</sup>Key Laboratory for Chemical Biology of Fujian Province, College of Chemistry and Chemical Engineering, Xiamen University, Xiamen, China; and <sup>4</sup>Department of Chemistry, College of Chemistry and Chemical Engineering, Xiamen University, Xiamen, China

**Abbreviations:** (AA) acrylic acid, (AAM) acrylamide, (EDC) N-(3-dimethylaminopropyl)-N'-ethyl-carbodiimide hydrochloride, (FPBA) 2-aminomethyl-5-fluorophenylboronic acid, (IFG) impaired fasting glucose, (NaOH) sodium hydroxide, (NIPAM) N-isopropylacrylamide, (NP) nanoparticle, (PBS) phosphate-buffered saline, (PL) photoluminescence, (QD) quantum dot, ( $R_h$ ) hydrodynamic radius, (UV-Vis) ultraviolet-visible, (ZnO) zinc oxide

**Keywords:** fluorescent, glucose sensor, hybrid nanogel, responsive, self-regulated insulin release

**Corresponding Author:** Weitai Wu, Ph.D., Department of Chemistry, College of Chemistry and Chemical Engineering, Xiamen University, Xiamen 361005, China; email address [wuwtxmu@xmu.edu.cn](mailto:wuwtxmu@xmu.edu.cn)

## Introduction

Hydrogel has attracted much attention because of its unique physical properties common to living tissues, including a soft and rubbery consistency and low interfacial tension with water or biological fluids.<sup>1</sup> While it has been possible to obtain glucose-responsive hydrogels within a considerable range, the lag time of bulk gels to reach swelling/collapsing equilibrium is thought to be the stumbling block to the realization of a gel-based closed-loop glycemic control system.<sup>2-4</sup> Theoretically, swelling/collapsing processes of gels are determined by the collective diffusion of the polymer networks in a fluid. The characteristic time period that describes the volume change of gels is approximately proportional to the square of the characteristic length of the gel.<sup>5,6</sup> Our group and other groups have predominantly improved the response speed by downsizing the glucose-responsive hydrogels into submicron and even nanogels.<sup>7-13</sup> In contrast to bulk hydrogels, the microgels/nanogels can be dispersed in water while preserving a highly stable structure. Moreover, with the inorganic quantum dots (QDs) or nanoparticles (NPs) being physically restricted in the polymer networks, the obtained inorganic-polymer hybrid microgels/nanogels could optically read out the glucose concentrations in aqueous solutions.<sup>10-12</sup>

The goal of this study is to develop a new class of inorganic-polymer hybrid nanogels comprising fluorescent zinc oxide (ZnO) QDs covalently bonding to boronate-derived nanogel network chains of poly[N-isopropyl-acrylamide (NIPAM)-co-acrylamide (AAm)-co-2-acrylamidomethyl-5-fluorophenylboronic acid (FPBA)] as the glucose recognition element. The newly designed hybrid nanogels are expected to possess improved sensitivity and selectivity for glucose sensing in blood samples. It is also expected that the glucose-responsive volume change of the hybrid nanogels can regulate the insulin release toward the construction of a closed-loop glycemic control system.

## Methods

### Materials

D(+)-Glucose, FPBA, and human serum albumin were purchased from ACROS, Combi-Blocks Inc., (San Diego, CA) and Tokyo Chemical Industry (Shanghai, China), respectively. Other chemicals were purchased from Aldrich. Azobisisobutyronitrile was recrystallized from anhydrous ethanol. N-isopropylacrylamide was recrystallized from a 1:1 hexane-acetone mixture. Acrylic acid (AA) was distilled under reduced pressure. The lyophilized insulin

from bovine pancreas (5.8 kDalton), zinc methacrylate, AAm, N,N'-methylenebisacrylamide, N-(3-dimethylamino-propyl)-N'-ethyl-carbodiimide hydrochloride (EDC), and other chemicals were used as received.

### Preparation of Zinc Oxide @ poly(N-Isopropylacrylamide -Acrylamide-2-Aminomethyl-5-Fluorophenylboronic Acid) Hybrid Nanogels

Zinc methacrylate (1.28 mmol), NIPAM (12.00 mmol), AAm (12.00 mmol), AA (12.00 mmol), and N,N'-methylenebisacrylamide (0.18 mmol) was dissolved in 25 ml anhydrous ethanol. The solution was stirred and heated to 80 °C, and then azobisisobutyronitrile (0.41 mmol) was added. After refluxing for 2 min, the solution turned milky white, and 0.25 ml 10.0 M sodium hydroxide (NaOH) aqueous solution was then added. The reaction system was continuously refluxed for 1 h. After cooling to room temperature, the obtained ZnO@poly(NIPAM-AAm-AA) hybrid nanogels were purified by centrifugation (20000 rpm, 30 min, 35 °C), redispersion in water, and 3 days' dialysis (cutoff 12,000-14,000) against water. Afterward, the FPBA moieties were coupled to form ZnO@poly(NIPAM-AAm-FPBA) hybrid nanogels using our previously reported procedure.<sup>10,11</sup> First, 0.231 g of FPBA and 0.230 g of EDC were dissolved in 35 ml water. After being cooled in an ice bath, 20 ml purified ZnO@poly(NIPAM-AAm-AA) hybrid nanogels were added to the solution. The reaction was kept for 6 h at 0 °C. The resultant products were purified by dialysis against very frequently changed water for at least 1 week.

### Glucose Sensing in Aqueous Solutions

The hybrid nanogels were adjusted to an appropriate concentration of 50.0 µg/ml for all measurements. To study the glucose-responsive optical properties, photoluminescence (PL) spectra of the hybrid nanogels were recorded in 5.0 mM phosphate-buffered saline (PBS) of pH = 7.4 at 37 °C and different glucose concentrations, in the absence and presence of specific interference constituents, respectively. The experiments were repeated five times at each glucose concentration, and the average intensity at 530 nm (*I*) was used for constructing the model. To simplify the calculation model, the PL intensity of the hybrid nanogels in PBS of pH = 7.4 without any sugar (*I*<sub>0</sub>) was used for normalization in all experiments.

### Glucose Sensing in Blood Serums

A representative sample of 11 adult diabetes patients

participated in this study. After overnight fasting, participants underwent an oral glucose-tolerance test. The impaired fasting glucose (IFG) was measured on an automatic chemistry analyzer using an enzyme-based method. For the tests using our hybrid nanogel as sensor, the PL intensity at 530 nm ( $I$ ) was recorded directly and repeated five times at each sample. The apparent IFG levels were read out based on the calibration model constructed from the PL reading of a series of hybrid nanogel dispersions in PBS of pH = 7.4 in the presence of different amounts of glucose with exactly known concentrations at 37°C, following the method described in the previous subsection.

### In Vitro Insulin Release Study

Insulin was loaded into the hybrid nanogels by the complexation method. After adjusting the pH to 9.0 with dilute NaOH solution, the hybrid nanogel dispersion (5.0 ml) was stirred in an ice water bath for 30 min, and 1.0 ml of insulin solution (1.0 mg/ml in PBS of pH = 7.4) was then added dropwise to the vial. The immediate clouding revealed the hydrogen bonding complexation of the -OH groups in the insulin molecules with the boronic acid groups in the hybrid nanogels. After stirring overnight, the insulin-loaded hybrid nanogel particles were then collected by centrifugation (37 °C, 6000 rpm, and 30 min) and washed by glucose solution (125.0 mg/dl) six times. All the upper clear solutions were collected. The concentration of free insulin was determined by ultraviolet-visible (UV-Vis) absorbance at 276 nm based on the linear calibration curve obtained from the standard solutions. The amount of loaded insulin in hybrid nanogels was calculated from the decrease in drug concentration, expressed as the mass of loaded drug per unit weight of dried hybrid nanogels.

The purified insulin-loaded nanogels were redispersed in PBS (5.0 ml, pH = 7.4) for *in vitro* drug release tests. A dialysis bag (cutoff 12,000–14,000) filled with 1.0 ml purified insulin-loaded hybrid nanogel dispersion was immersed in 50 ml PBS of pH = 7.4 at 37.0 °C and various glucose concentrations. The released insulin outside the dialysis bag was sampled at defined time intervals and assayed by UV-Vis absorbance at 276 nm. Cumulative release is expressed as the total percentage of drug released through the dialysis membrane over time. The evolution of release kinetics in response to glucose concentration changes was also monitored.

### Characterizations

Ultraviolet-visible absorption spectra were obtained on a Helios  $\beta$  Spectrophotometer (Thermo Electron Co.,

Swedesboro, NJ). The PL spectra of the hybrid nanogel dispersions at different glucose concentrations were obtained on a FluoroMax<sup>®</sup>-3 Spectrofluorometer (Jobin Yvon Co., Edison New Jersey, NJ). Transmission electron microscope images were taken on a FEI TECNAI (Hillsboro, OR) transmission electron microscope at an accelerating voltage of 120 kV. Dynamic light scattering was performed on a BIC 90Plus multiangle particle sizing analyzer (Brookhaven Instruments Corporation, Holtsville, NY) with a He-Ne laser (35 mW, 659 nm) as light source to measure the hydrodynamic radius ( $R_h$ ) distributions at a scattering angle  $\theta = 90^\circ$ . Impaired fasting glucose measurements were carried out on a CX9 Chemistry Analyzer (Beckman Coulter, Brea, CA).

## Results

### Preparation of Zinc Oxide @ poly(N-Isopropylacrylamide -Acrylamide-2-Aminomethyl-5-Fluorophenylboronic Acid) Hybrid Nanogels

Following the main objective to probe glucose level and deliver insulin (**Figure 1**), our strategy was to integrate the glucose recognition elements and fluorescent components into a single nanogel. We first synthesized the ZnO@poly(NIPAM-AAm-AA) hybrid nanogels ( $80 \pm 20$  nm; **Figure 2A**) with the fluorescent ZnO QDs covalently bonding to the copolymer nanogel network chains.<sup>14,15</sup> The glucose recognition moieties FPBA were then coupled to the carboxyl groups of AA units in the hybrid nanogels under EDC catalysis to yield ZnO@poly(NIPAM-AAm-FPBA) hybrid nanogels ( $50 \pm 20$  nm; **Figure 2B**). The infrared spectra indicated that the

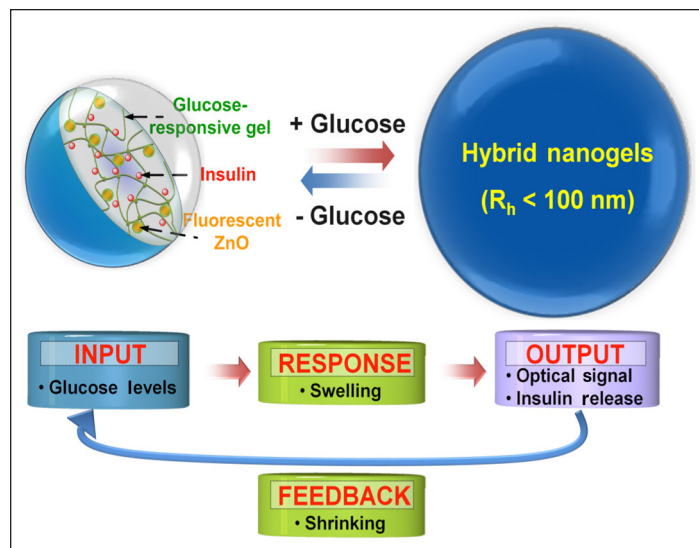


**Figure 1.** Schematic illustration of a single hybrid nanogel for integration of fluorescent glucose sensing and insulin delivery.



glucose receptors were successfully coupled (Figure 3). The resultant ZnO@poly(NIPAM-AAm-FPBA) hybrid nanogels exhibited strong absorption and PL intensity (Figure 4) and were very stable. No sediment was observed, and only a marginal change in UV-Vis spectrum could be detected (Figure 4A) after 3 months' storage at room temperature. This result indicates that the polymer network is fine enough to immobilize ZnO QDs stably to prevent relocalization, aggregation, or leakage of the QDs in the hybrid nanogels.

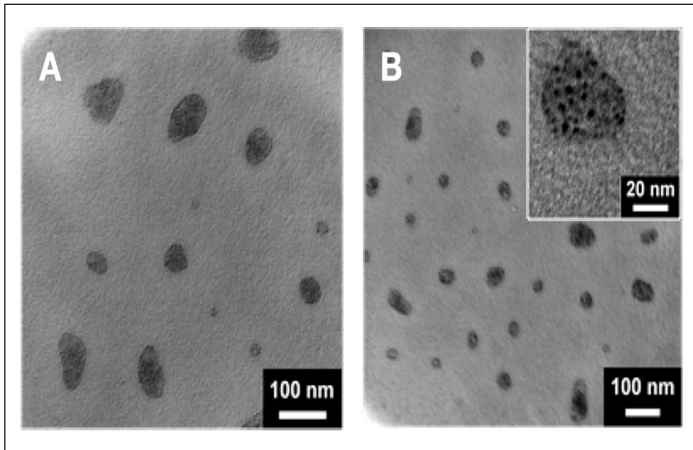


**Figure 2.** Transmission electron microscope images of (A) ZnO@poly(NIPAM-AAm-AA) and (B) ZnO@poly(NIPAM-AAm-FPBA) hybrid nanogels dried from the PBS of pH = 7.4.

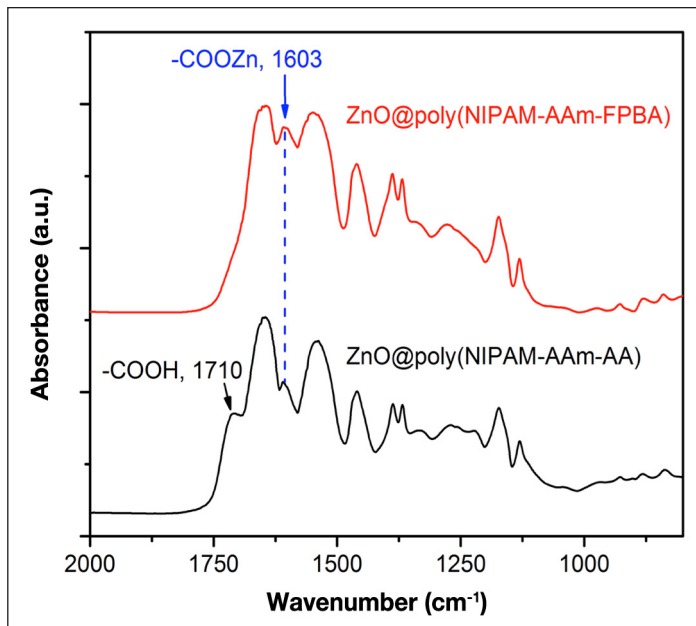


**Figure 3.** Infrared spectra of ZnO@poly(NIPAM-AAm-AA) and ZnO@poly(NIPAM-AAm-FPBA) hybrid nanogels, indicating a successful coupling of FPBA to the -COOH groups in the ZnO@poly(NIPAM-AAm-AA) hybrid nanogels.

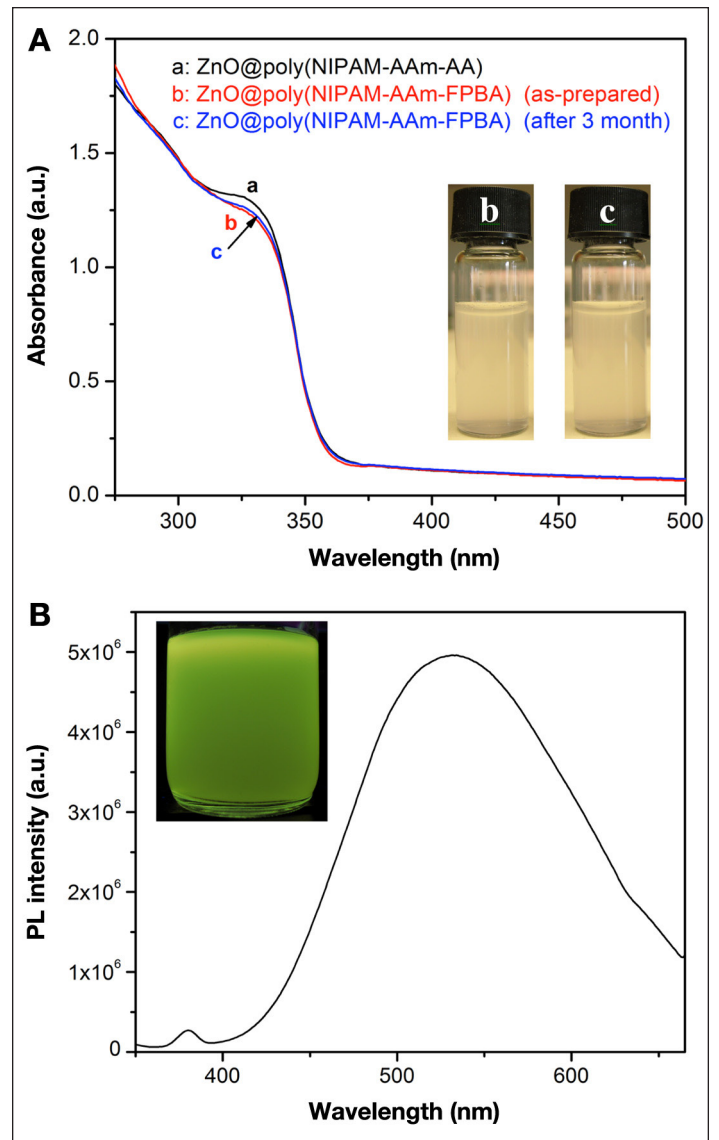


**Figure 4.** (A) The UV-Vis absorption and (B) PL spectra of ZnO@poly(NIPAM-AAm-FPBA) hybrid nanogels. Digital photographs inset in (A) show the stability without sediment of the hybrid nanogel dispersion. The photograph inset in (B) was taken under a 375 nm ultraviolet lamp. The UV-Vis absorption spectrum of ZnO@poly(NIPAM-AAm-AA) hybrid nanogels was also shown in (A) for comparison.

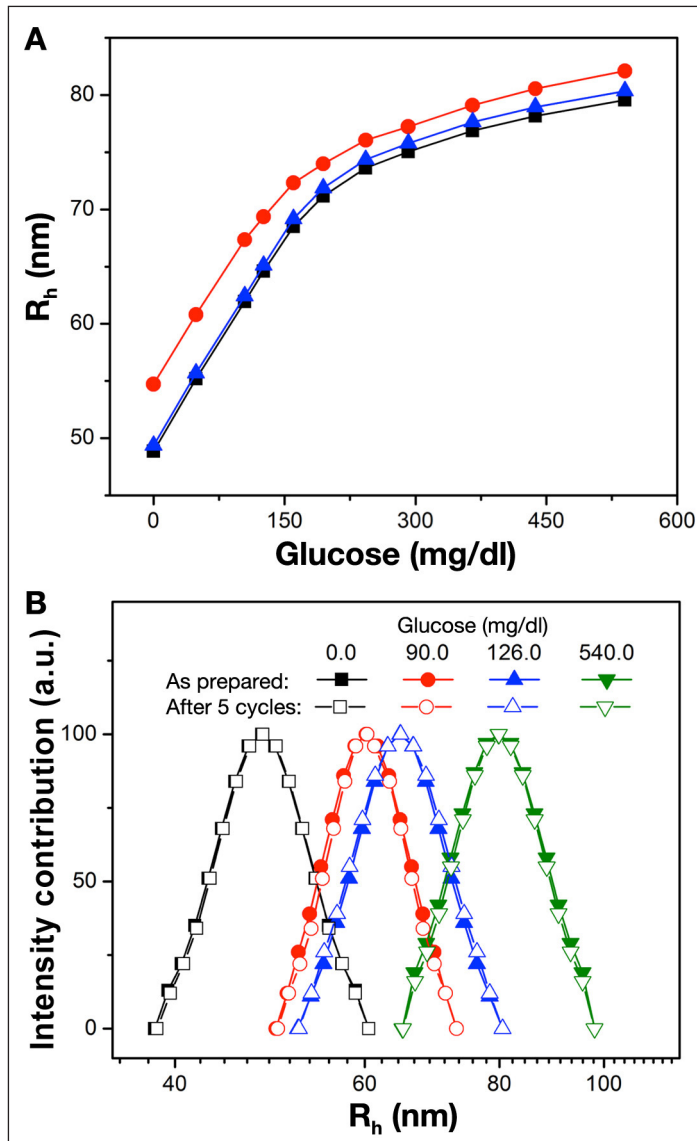
### Glucose Sensing in Aqueous Solutions

Figure 5A shows the glucose-induced swelling curve of ZnO@poly(NIPAM-AAm-FPBA) hybrid nanogels over the clinically relevant glucose concentration range of 18–540 mg/dl. The high swelling ratio ( $R_{h,540 \text{ mg/dl}}/R_{h,0 \text{ mg/dl}} = 1.63$ ) demonstrated a high sensitivity of these hybrid nanogels to glucose. The covalent bonds formed between boronic acid and *cis*-diols are reversible.<sup>16</sup> As glucose is removed from the bathing medium by dialysis against very frequently changed water, the

dissociation equilibrium shifts back from boronate ester to boronic acid, leading to an almost full recovery of the size distribution curve of nanogels (**Figure 5B**) even after five cycles of repeated glucose addition and removal, which is crucial for quantitative applications. The addition of L-lactate ( $2.0 \times 10^{-2}$  mol/liter) or D(+)-galactose ( $1.0 \times 10^{-4}$  mol/liter) led to a slightly higher glucose-induced swelling of the hybrid nanogels (within  $\pm 10\%$ ). In addition, the glucose-responsive volume change of the hybrid nanogels was relatively independent of the

surrounding temperature ( $\sim 22\text{--}38$  °C) and pH (5.0–7.6) change (**Figure 6**), which is another important feature of this sensor for further application.

The glucose-responsive nanogel can modify the physico-chemical environment of the embedded QDs,<sup>10–12,17</sup> converting the disruptions in homeostasis of glucose level into optical signals (**Figures 7A** and **7B**). In comparison with the glucose-induced swelling curve (**Figure 5A**), the quenched PL intensity ( $100 - 100 \times I_{[\text{Glucose}]} / I_0$  mg/dl)



**Figure 5.** (A) Glucose concentration (glucose) dependent average  $R_h$  values of ZnO@poly(NIPAM-AAm-FPBA) hybrid nanogels in PBS of pH = 7.4 (squares), PBS of pH = 7.4 with  $2.0 \times 10^{-2}$  mol/liter L-lactate (circles), and PBS of pH = 7.4 with  $1.0 \times 10^{-4}$  mol/liter D(+)-galactose (triangles), respectively. (B) Size distributions of the hybrid nanogels at different glucose concentrations before and after five cycles of repeated addition and removal of glucose. All measurements were made at 37.0 °C.

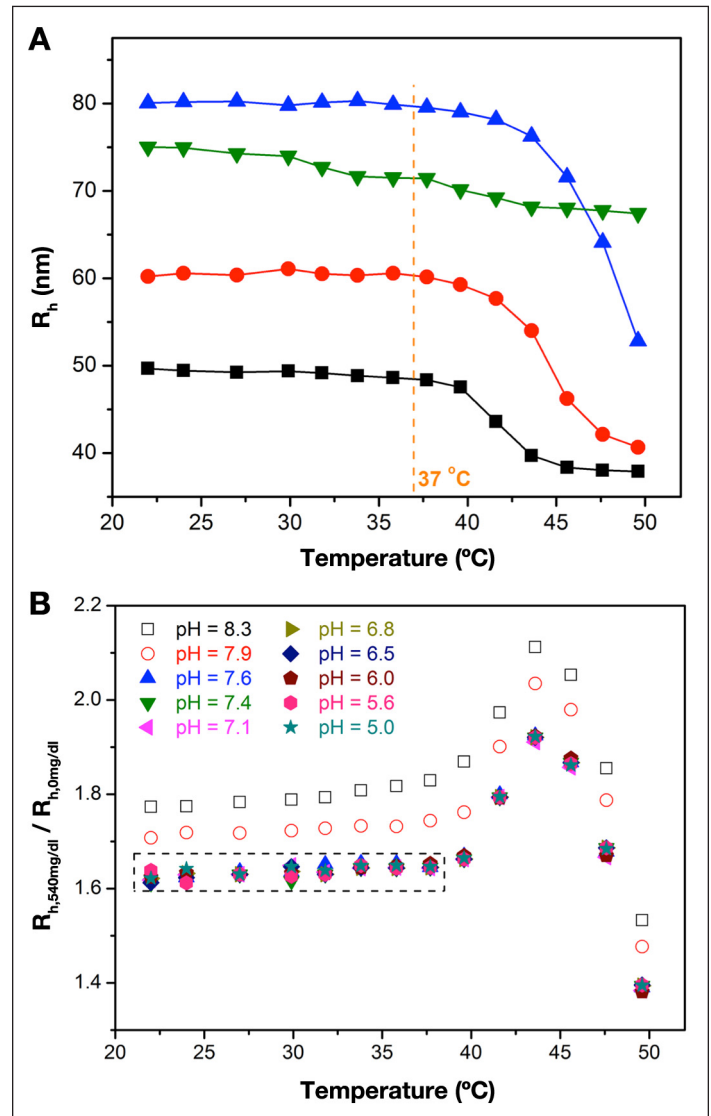


**Figure 6.** (A) Temperature-dependent average  $R_h$  values of ZnO@poly(NIPAM-AAm-FPBA) hybrid nanogels in PBS of pH = 7.4 with glucose concentrations of 0.0 mg/dl (squares), 90.0 mg/dl (circles), and 540.0 mg/dl (upright triangles). Dynamic light scattering data of ZnO@poly(NIPAM-AAm-AA) hybrid nanogels in PBS of pH = 7.4 was also presented for comparison (inverted triangles). (B) Temperature-dependent swelling ratio,  $R_h$ , 540 mg/dl/ $R_h$ , 0 mg/dl, of ZnO@poly(NIPAM-AAm-FPBA) hybrid nanogels in PBS of different pH values.

reveals nearly the same trend toward the glucose concentration change (**Figure 7C**), clearly correlating the glucose-responsive volume change of the nanogel to the PL response of the ZnO QDs immobilized in the nanogel. The linear plot (**Figure 7D**) of the glucose-responsive PL property in reciprocal space gives the relationship in a more orthogonal fashion. The detection limit is estimated to be  $\pm 1.7$  mg/dl. The relative error of glucose concentration reading (18.0–540.0 mg/dl) in the presence of common nonglucose constituents<sup>18</sup> found in biological systems is generally within  $\pm 7.8\%$  after taking account of

the experimental errors (**Table 1**). Similar to the glucose-responsive volume change, the glucose reading of the hybrid nanogels is also relatively independent of the surrounding change in temperature range of  $\sim 22$ – $38$  °C and pH range of 5.0–7.6. Only  $\pm 0.9\%$  change was detected for the glucose reading in this temperature range.

### Glucose Sensing in Blood Serums

To further confirm the high selectivity of the ZnO@poly(NIPAM-AAm-FPBA) hybrid nanogel sensor, blood

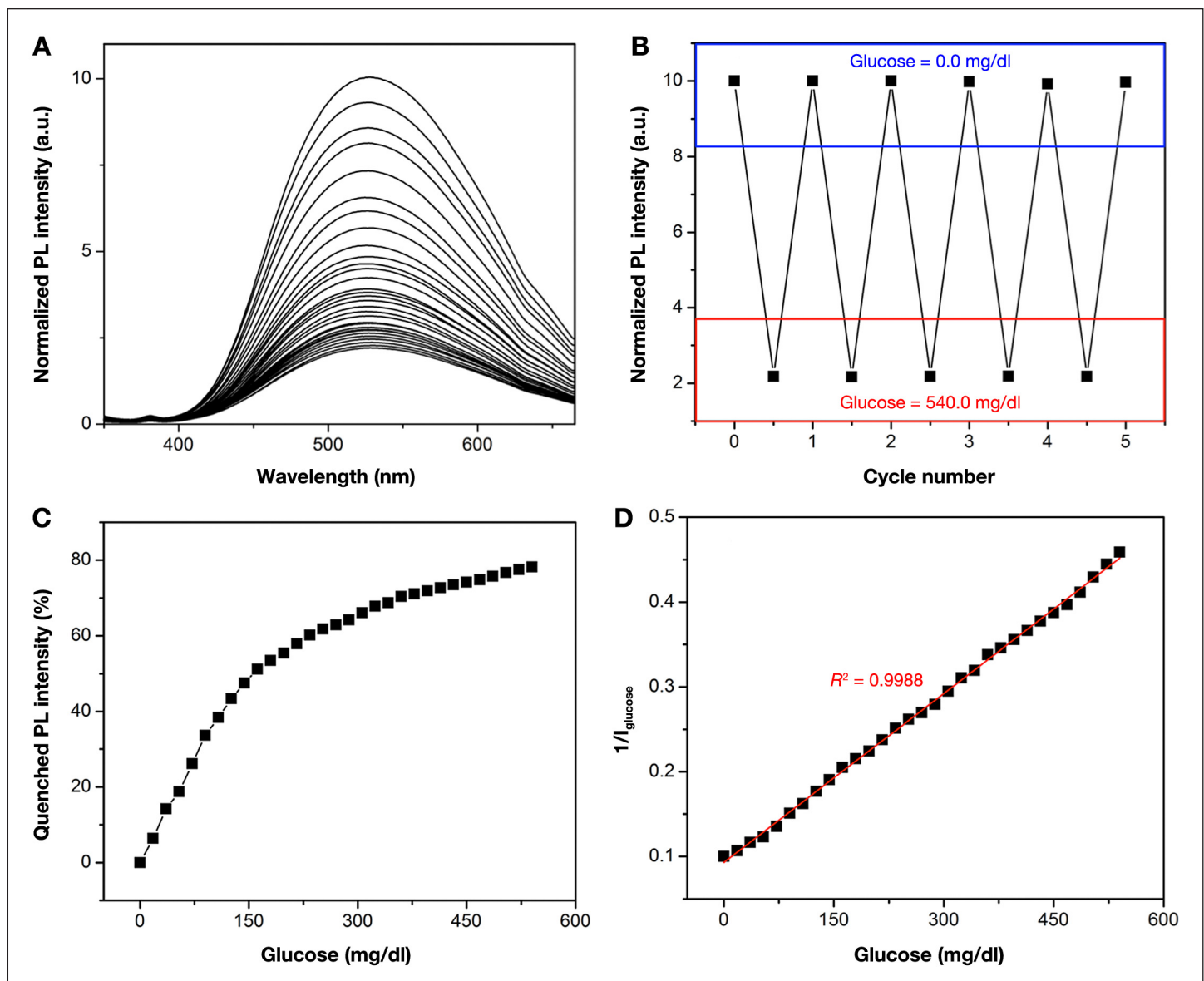


**Figure 7.** (A) Typical evolution of the PL spectra of ZnO@poly(NIPAM-AAm-FPBA) hybrid nanogels in response to a gradual increase in glucose. Scans were taken from 0 (top) to 540.0 mg/dl (bottom) with an interval of 18.0 mg/dl. (B) The PL quenching and recovery cycles upon the repeated addition (540.0 mg/dl) and dialysis removal of glucose (0.0 mg/dl) in the dispersion medium of the hybrid nanogels. (C) Quenched PL intensity at 530 nm as a function of glucose. (D) Linear plot showing the glucose-responsive PL intensity (normalized) in the reciprocal space. All measurements were made in PBS of pH = 7.4 at 37.0 °C. Excitation wavelength = 340 nm.

**Table 1.**  
Interferences of Various Common Nonglucose Constituents Found in Biological Systems

Constituents	Concentration	Relative error <sup>a</sup>
Human serum albumin	44.0 g/liter	+5.3
L-lactate	$2.0 \times 10^{-2}$ mol/liter	+7.8
D(-)-fructose	$1.0 \times 10^{-4}$ mol/liter	+1.9
D(+)-galactose	$1.0 \times 10^{-4}$ mol/liter	+0.8
D(+)-mannose	$1.0 \times 10^{-4}$ mol/liter	+0.6
Pyruvic acid	$1.0 \times 10^{-4}$ mol/liter	+0.3
K <sup>+</sup>	$2.0 \times 10^{-3}$ mol/liter	-0.1
Na <sup>+</sup>	$2.0 \times 10^{-3}$ mol/liter	-0.1
Ca <sup>2+</sup>	$2.0 \times 10^{-2}$ mol/liter	-0.3
Mg <sup>2+</sup>	$5.0 \times 10^{-4}$ mol/liter	-0.3
Ba <sup>2+</sup>	$2.0 \times 10^{-3}$ mol/liter	-1.0
Al <sup>3+</sup>	$5.0 \times 10^{-5}$ mol/liter	-0.5
Cu <sup>2+</sup>	$2.0 \times 10^{-6}$ mol/liter	-0.9
Zn <sup>2+</sup>	$5.0 \times 10^{-5}$ mol/liter	-0.3
Co <sup>2+</sup>	$5.0 \times 10^{-6}$ mol/liter	-1.1
Fe <sup>3+</sup>	$2.0 \times 10^{-6}$ mol/liter	-0.7
Urea	$5.0 \times 10^{-5}$ mol/liter	-2.2
Citric acid	$5.0 \times 10^{-5}$ mol/liter	+1.2
Vitamin C	$5.0 \times 10^{-5}$ mol/liter	+2.9
$\gamma$ -globulins	$5.0 \times 10^{-5}$ mol/liter	+1.8
Lysozyme	$5.0 \times 10^{-5}$ mol/liter	+1.3
Glycine	$1.0 \times 10^{-4}$ mol/liter	-1.3
Arginine	$1.0 \times 10^{-4}$ mol/liter	-1.0
L-phenylalanine	$1.0 \times 10^{-4}$ mol/liter	+2.6
Lysine	$1.0 \times 10^{-4}$ mol/liter	+1.5
L-cysteine	$5.0 \times 10^{-4}$ mol/liter	+3.5
Tyrosine	$5.0 \times 10^{-4}$ mol/liter	-1.6
Cholesterol	$1.0 \times 10^{-5}$ mol/liter	+2.8

<sup>a</sup> "+" and "-" indicate an increase and decrease in glucose-induced PL quenching, respectively.

serums of 11 adults with diabetes were adopted as the subject of the hybrid nanogels. With the curves in **Figures 7C** and **7D** obtained in PBS of pH = 7.4 as the calibration curves, the apparent IFG of the blood samples could be obtained from the PL reading, which was compared with the corresponding actual IFG levels measured in-hospital by using an enzyme-based method. The apparent IFG levels were generally higher than the actual IFG levels (**Figure 8**), with a larger deviation appearing at a higher IFG level (deviation ratio  $\leq +11.2\%$ ). Reading error in the calibration and sample sets was

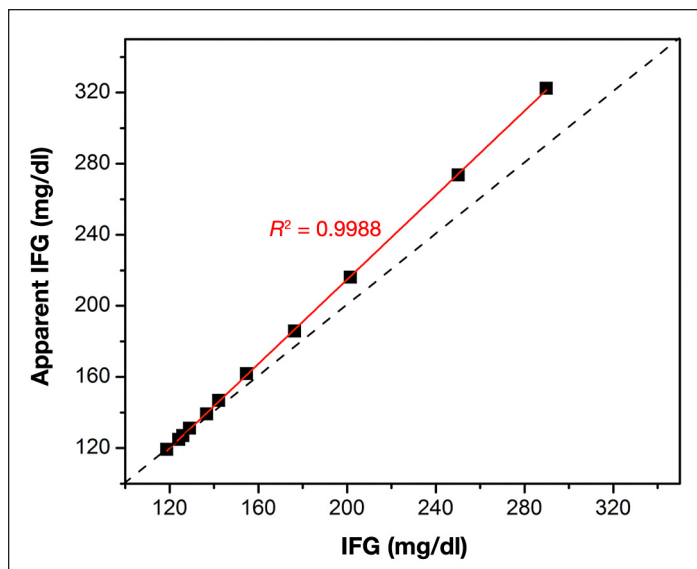


**Figure 8.** Comparison of the actual IFG obtained in-hospital by using an enzyme-based method and the apparent IFG predicted with ZnO@poly(NIPAM-AAm-FPBA) hybrid nanogels as glucose sensors for the same blood serum samples. The error bars are within the symbols.

determined by calculating the root-mean-squared error of apparent IFG:

$$\text{RMSEC}(n) = \sqrt{\frac{\sum_{i=1}^n (\text{IFG}_{\text{apparent}} - \text{IFG})_i^2}{n}}$$

Clearly, the hybrid nanogels revealed slightly large root-mean-squared error of apparent IFG (11) values of 14.1 mg/dl in glucose reading, corresponding to an average of 14.1 mg/dl higher in the apparent IFG than the actual IFG.

### In Vitro Insulin Release Study

The porous network structure of gel is particularly well suited to trap insulin, resulting in a high loading capacity of 58.1 wt%, which is equivalent to  $\sim 752.1$  IU/liter after taking account of the typical concentrations of hybrid nanogel dispersions. As shown in **Figure 9A**, the glucose-responsive volume phase transition of the hybrid nanogels can regulate the release of the preloaded insulin. The much slower insulin release from the hybrid nanogels compared with that from the free insulin solution indicates a sustained release process. The higher the glucose level ( $\geq 126.0$  mg/dl in diabetes patients), the more insulin the hybrid nanogels can deliver, standing in vivid contrast with the low release efficiency at normal glucose level (only  $\sim 5\%$  released at 108.0 mg/dl in 76 h). The coexistence of L-lactate ( $2.0 \times 10^{-2}$  mol/liter) or D(+)-galactose ( $1.0 \times 10^{-4}$  mol/liter) can lead to a slightly higher glucose-induced release of insulin (within  $\pm 6\%$ , **Figure 9B**).



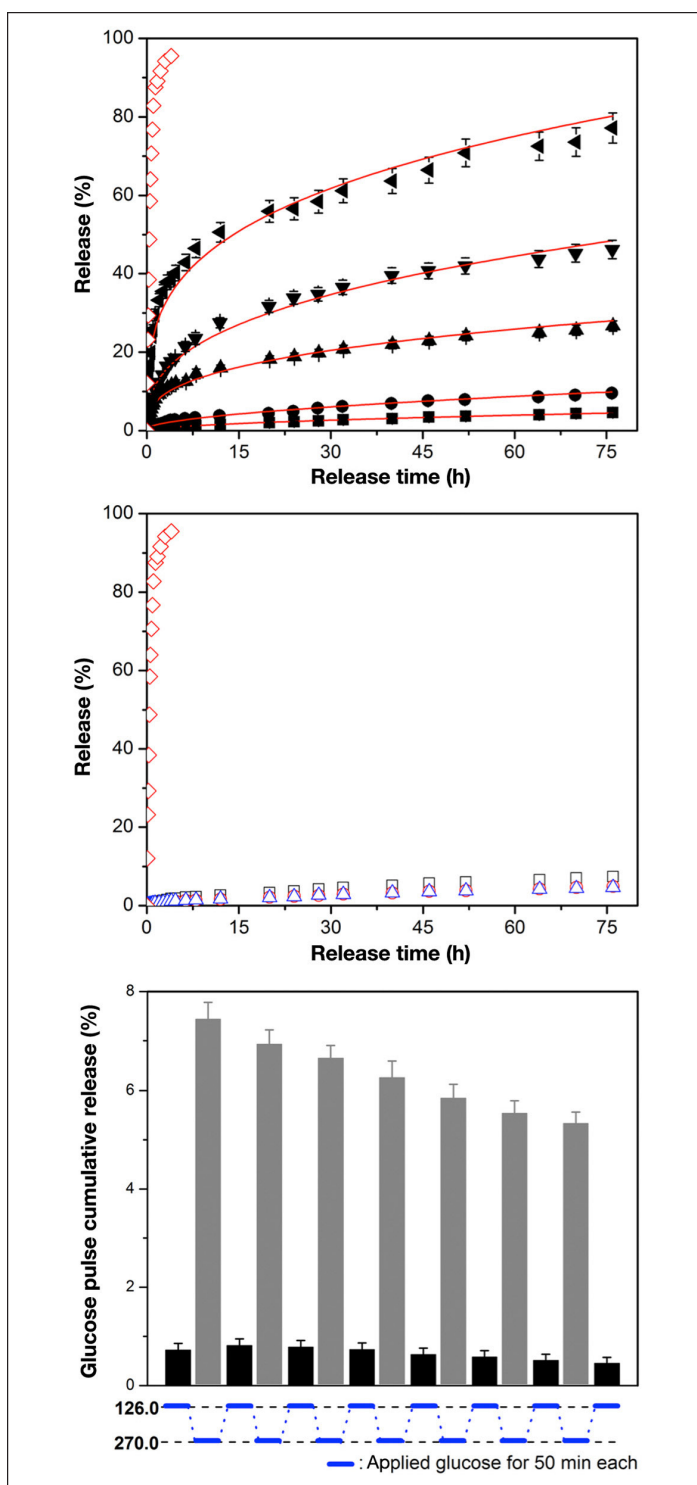


**Figure 9.** (A) Releasing profiles of insulin from ZnO@poly(NIPAM-AAm-FPBA) hybrid nanogels in the presence of 90.0 mg/dl (squares), 126.0 mg/dl (circles), 180.0 mg/dl (upright triangles), 270.0 mg/dl (inverted triangles), and 360.0 mg/dl (sideways triangles) glucose in PBS of pH = 7.4 at 37.0 °C. The blank release (diamonds in B) represents the release of insulin from the free insulin solution in the same PBS. (B) Control experiments with no glucose (squares), with 90.0 mg/dl glucose plus  $2.0 \times 10^{-2}$  mol/liter L-lactate (circles), and with 90.0 mg/dl glucose plus  $1.0 \times 10^{-4}$  mol/liter D(+)-galactose (triangles), respectively. (C) Insulin release from the hybrid nanogels by stepwise treatment with 126.0 and 270.0 mg/dl glucose. Glucose was introduced every 50 min and removed by PBS washing 10 min post-treatment.

Moreover, the insulin release profile exhibited a pulsed appearance when the glucose level was alternatively changed between 126.0 and 270.0 mg/dl (Figure 9C), showing that the drug release from the hybrid nanogels could be switched on and off repeatedly in response to the glucose level fluctuation, which demonstrates a great promise for the closed-loop control of glucose.

## Discussion

To this end, we have developed a new class of inorganic-polymer ZnO@poly(NIPAM-AAm-FPBA) hybrid nanogels to integrate the glucose-receptor (FPBA groups herein) and fluorescent components (ZnO QDs herein) into a single nanogel that can carry insulin drugs. The FPBA groups not only have a low  $pK_a$  (close to physiological pH) due to the presence of electron-withdrawing fluorine,<sup>19</sup> but also diminish interference due to the selective binding of the 2-acrylamidophenylboronate to glucose over nonglucose constituents.<sup>20</sup> Thus the FPBA functionalized hybrid nanogels are expected to bind glucose sensitively and selectivity in physiological solution, which would increase the charge density and build up a Donnan potential for the gel to swell steadily with an increase in glucose level over the clinically relevant glucose concentration range of 18–540 mg/dl (Figure 5). The reversible glucose-responsive volume change of the gel can modify the physicochemical environment of the embedded ZnO QDs and thus convert the disruptions in homeostasis of glucose level into highly reproducible fluorescent signals (Figures 7 and 8), providing optical readout of the glucose level in blood samples. In comparison with our previously studied hybrid nanogels with the QDs/NPs physically restricted in the polymer networks,<sup>10–12</sup> the ZnO@poly(NIPAM-AAm-FPBA) hybrid nanogels with ZnO QDs covalently bonding to the gel network chains demonstrate a much higher sensitivity of PL response, possibly due to the rapid and sensitive transmission of the elastic tension directly from the polymer chains to the covalently bonded QDs. The rapid and highly accurate PL response of the sensor is necessary for future *in situ* studies in biosystems.

The glucose-responsive volume phase transition of the hybrid nanogels can further regulate the release of the preloaded insulin (Figure 9). The releasing profiles showed that the insulin release at a normal glucose level (108.0 mg/dl) is the slowest. As the glucose level gradually increases, insulin is released at faster rates because of the gradual swelling of gel network (larger mesh size). Ideal insulin delivery carriers should keep the loaded



insulin minimally released at normal glucose levels but release rapidly upon reaching hyperglycemia to control glucose levels.<sup>21,22</sup> The glucose-responsive insulin release clearly confers the advantages of the hybrid nanogels as delivery carriers. Moreover, the insulin release can be switched on and off by alternatively changing the glucose level between 270.0 and 126.0 mg/dl, further demonstrating the potential applicability of this drug delivery system.

Clearly, the discussed results, in terms of the glucose-responsive volume phase transition, PL property change, and insulin releasing rate, provide a good and fairly accurate account for the closed-loop glycemic control ability of the newly designed ZnO@poly(NIPAM-AAm-AA) hybrid nanogels. However, the current results are obtained from *in vitro* physicochemical studies. More studies are required to further improve the hybrid nanogel systems for potential *in vivo* applications. For example, the composition and structure of the polymer nanogels need be further optimized to provide a broad range of insulin loading capacity and glucose-responsive insulin releasing rate to ensure that the nanogel releases the correct amount of insulin corresponding to different particular glucose levels in the physiologically important glucose concentration range. New inorganic QDs or NPs with low toxicity and strong emission in the near-infrared wavelength range need be developed and immobilized into the nanogels for *in vivo* continuous glucose detection. Methods need be developed as to how and where these hybrid nanogels will be implanted or deployed in the body. Nevertheless, the *in vitro* physicochemical exercises of the novel hybrid nanogel for continuous glucose detection and glucose-responsive insulin release have set a good starting point for the development of new glucose sensors and insulin delivery carriers toward the ultimate use in diabetes management.

## Conclusions

We have designed a new class of inorganic-polymer hybrid nanogels, which can adapt to glucose levels with high sensitivity and selectivity in blood samples, for potential closed-loop control of glucose. The glucose-responsive behavior of the new hybrid nanogels is generally comparable and, in some cases, superior to the arts reported previously with the QDs/NPs physically restricted in the polymer networks. A single hybrid nanogel acting as a monitoring system (glucose sensor) that evaluates an input (glucose levels) and simultaneously uses a control system to predictably control the output (insulin infusion rate). These physicochemical exercises

are promising, but further optimization of the system and true physiological studies are crucial developmental steps toward the ultimate use in diabetes management.

---

### Funding:

This work was supported by the American Diabetes Association (Basic Science Award 1-12-BS-243). The research carried out in China was supported by the Xiamen University Start-Up Fund (985 Project) and the National Foundation for Fostering Talents of Basic Science (J1030415).

---

### References:

1. Peppas NA, Hilt JZ, Khademhosseini A, Langer R. Hydrogels in biology and medicine: from molecular principles to bionanotechnology. *Adv Mater*. 2006;18:1345–60.
2. Shiino D, Murata Y, Kubo A, Kim YJ, Kataoka K, Koyama Y, Kikuchi A, Yokoyama M, Sakurai Y, Okano T. Amine containing phenylboronic acid gel for glucose-responsive insulin release under physiological pH. *J Control Release*. 1995;37:269–76.
3. Wu JY, Liu SQ, Heng PW, Yang YY. Evaluating proteins release from, and their interactions with, thermosensitive poly (N-isopropylacrylamide) hydrogels. *J Control Release*. 2005;102(2):361–72.
4. Siegel RA, Gu Y, Lei M, Baldi A, Nuxoll EE, Ziaie B. Hard and soft micro- and nanofabrication: an integrated approach to hydrogel-based biosensing and drug delivery. *J Control Release*. 2010;141(3):303–13.
5. Li Y, Tanaka T. Kinetics of swelling and shrinking of gels. *J Chem Phys*. 1990;92(2):1365–71.
6. Reese CE, Mikhonin AV, Kamenjicki M, Tikhonov A, Asher SA. Nanogel nanosecond photonic crystal optical switching. *J Am Chem Soc*. 2004;126(5):1493–6.
7. Zhang Y, Guan Y, Zhou S. Synthesis and volume phase transitions of glucose-sensitive microgels. *Biomacromolecules*. 2006;7(11):3196–201.
8. Zhang Y, Guan Y, Zhou S. Permeability control of glucose-sensitive nanoshells. *Biomacromolecules*. 2007;8(12):3842–7.
9. Wu W, Zhou T, Aiello M, Zhou S. Optically pH and H<sub>2</sub>O<sub>2</sub> dual responsive composite colloids through the directed assembly of organic dyes on responsive microgels. *Chem Mater*. 2009;21:4905–13.
10. Wu W, Zhou T, Shen J, Zhou S. Optical detection of glucose by CdS quantum dots immobilized in smart microgels. *Chem Commun (Camb)*. 2009;29:4390–2.
11. Wu W, Zhou T, Aiello M, Zhou S. Construction of optical glucose nanobiosensor with high sensitivity and selectivity at physiological pH on the basis of organic-inorganic hybrid microgels. *Biosens Bioelectron*. 2010;25(12):2603–10.
12. Wu W, Mitra N, Yan EC, Zhou S. Multifunctional hybrid nanogel for integration of optical glucose sensing and self-regulated insulin release at physiological pH. *ACS Nano*. 2010;4(8):4831–9.
13. Chen MC, Sonaje K, Chen KJ, Sung HW. A review of the prospects for polymeric nanoparticle platforms in oral insulin delivery. *Biomaterials*. 2011;32(36):9826–38.
14. Xiong HM, Xu Y, Ren QG, Xia YY. Stable aqueous ZnO@polymer core-shell nanoparticles with tunable photoluminescence and their application in cell imaging. *J Am Chem Soc*. 2008;130(24):7522–3.
15. Wu W, Shen J, Banerjee P, Zhou SQ. A multifunctional nano-platform based on responsive fluorescent plasmonic ZnO-Au@PEG hybrid nanogels. *Adv Funct Mater*. 2011;21:2830–9.

16. Davis AP, Wareham RS. Carbohydrate recognition through noncovalent interactions: a challenge for biomimetic and supramolecular chemistry. *Angew Chem Int Ed Engl.* 1999;38(20):2978–96.
17. Smith AM, Mohs AM, Nie S. Tuning the optical and electronic properties of colloidal nanocrystals by lattice strain. *Nat Nanotechnol.* 2009;4(1):56–63.
18. Burtis CA, Ashwood ER. *Tietz textbook of clinical chemistry.* 3rd ed. Philadelphia: WB Saunders; 1999.
19. Kabilan S, Marshall AJ, Sartain FK, Lee MC, Hussain A, Yang X, Blyth J, Karangu N, James K, Zeng J, Smith D, Domschke A, Lowe CR. Holographic glucose sensors. *Biosens Bioelectron.* 2005;20(8):1602–10.
20. Yang X, Lee MC, Sartain F, Pan X, Lowe CR. Designed boronate ligands for glucose-selective holographic sensors. *Chemistry.* 2006;12(33):8491–7.
21. Youssef JE, Castle J, Ward WK. A review of closed-loop algorithms for glycemic control in the treatment of type 1 diabetes. *Algorithms.* 2009; 2(1): 518–32.
22. Steiner MS, Duerkop A, Wolfbeis OS. Optical methods for sensing glucose. *Chem Soc Rev.* 2011;40(9):4805–39.